

INTERNATIONAL SOCIETY FOR SOIL MECHANICS AND GEOTECHNICAL ENGINEERING



This paper was downloaded from the Online Library of the International Society for Soil Mechanics and Geotechnical Engineering (ISSMGE). The library is available here:

<https://www.issmge.org/publications/online-library>

This is an open-access database that archives thousands of papers published under the Auspices of the ISSMGE and maintained by the Innovation and Development Committee of ISSMGE.

Interpretation of Liquefaction Field Case Histories for Use in Developing Liquefaction Triggering Curves

R. A. Green¹, S. M. Olson²

ABSTRACT

Case histories are central to developing liquefaction triggering curves. Interpreting case histories is inherently a forensic study where the researcher evaluates ground response during the causative earthquake using limited evidence collected after the event. For most cases, the evidence is limited to observations of surficial manifestations of liquefaction and in-situ test data. Based on this information, sites are classified as either “liquefied” or “not liquefied,” and a “critical layer” is selected. This paper reviews the standard practice for interpreting liquefaction case histories, and proposes interpretation guidelines that are based on consistency between the mode and severity of observed surficial manifestations and characteristics of the assumed critical layer. Two field case histories are used to illustrate the authors’ proposed guidelines for interpreting near level-ground triggering case histories, one from a modern earthquake and one from a paleoearthquake.

Introduction

In the broadest sense, a liquefaction triggering case history entails both “response” and “demand” components (e.g., post-event field observations and the associated seismic loading). Key to interpreting response for level- or mildly sloping-ground sites is characterizing the relevant soil properties. However, most often, the soil profile and corresponding properties are determined after the earthquake; and the seismic loading is estimated, rather than recorded, at the case history site. Also, only post-event observations at a given point in time are available for most cases, rather than a detailed description of response from the start of shaking to the end of deformations. Furthermore, most of the observations are of surface manifestations, not of the subgrade soil response. As a result, interpreting these field observations inherently involves a forensic analysis that requires considerable judgment. Not surprisingly, experienced investigators often produce differing interpretations from the same field observations. Regardless, the general consensus among the profession is that well-documented “case histories” are highly valuable.

In reviewing liquefaction triggering case history databases, several issues regarding how case histories were interpreted by various investigators emerge, including: (1) classification of “liquefied,” “not liquefied,” or “marginally liquefied” (i.e., “yes,” “no,” or “yes/no” cases, respectively); (2) selection of the “critical layer” (defined in detail subsequently) and its representative properties; (3) interdependence in the case histories; and (4) determination of the seismic demand. This paper focuses on the selection of the “critical layer” and its representative

¹Prof., Dept. of Civil and Environmental Engineering, Virginia Tech, Blacksburg, VA, USA, rugreen@vt.edu

²Assoc. Prof., Dept. of Civil and Env. Eng., Univ. of Illinois Urbana-Champaign, Urbana, IL, USA, olsons@illinois.edu

properties, which ultimately results in a data point that is used to develop level-ground liquefaction triggering curves, or cyclic resistance ratio (CRR) curves, which are empirical correlations relating soil liquefaction resistance to an in-situ test index (e.g., normalized standard penetration test blow count, cone penetration test tip resistance, or small strain shear wave velocity) (e.g., Whitman, 1971; Seed and Idriss, 1971).

In this paper, the authors first discuss background information on how the critical layers and representative properties were determined for cases in assembled databases. This is followed by guidelines proposed by the authors for interpreting case histories. Finally, two case histories are presented that illustrate the implementation of the authors' proposed guidelines.

Background

One of the first, if not the first, liquefaction triggering case history databases was assembled by Whitman (1971), which consisted of 13 different cases from 8 different earthquakes in Japan, Chile, U.S., Mexico, and the Philippines. Shortly thereafter, a larger database was assembled by Seed and Idriss (1971), which consisted of 35 cases from 12 earthquakes in Japan, U.S., and Chile. Among other descriptions of the compiled cases, both Whitman (1971) and Seed and Idriss (1971) listed the representative standard penetration test (SPT) N-values for the "critical layers." Although neither study gave an explicit definition of what the "critical layer" is, both studies inherently implied that the critical layer in the profile is the layer that liquefied for a "yes" cases. As a corollary, it is assumed that for the "no" cases, the critical layer is the layer that would have liquefied had the intensity of shaking been higher. Seed and Idriss (1971) did not state how they determined the specific critical layers, and Whitman (1971) gave only very limited insight in this regard: "*Various indicators of the critical depth were used: any evidence of the actual depth of liquefaction, the bottom of a shallow depth of granular material, and the depth of any sharp increase in penetration resistance.*" In both studies, it is clear that a great deal of judgment was used to select critical layers.

The Whitman (1971) and Seed and Idriss (1971) databases set the stage for subsequent databases. In many of these, multiple critical layers were selected from a single boring/sounding (e.g., Yegian and Vitelli, 1981; Tokimatsu and Yoshimi, 1983; Seed et al., 1984; Stark and Olson, 1995), yielding multiple data points for a given profile and causative earthquake that were then used to develop CRR curves. However, this practice generally has been avoided in more recent databases, where the "weakest-link-in-the-chain" concept has been used to select a single critical layer in a profile (e.g., Cetin et al., 2000; Moss, 2003; Idriss and Boulanger, 2008; Kayen et al., 2013; Boulanger and Idriss, 2014). For "yes" cases, the critical layer has sometimes been selected by comparing soil ejecta from surficial liquefaction manifestations to samples obtained from borings, when such data is available (e.g., Liao and Whitman, 1986; Green et al., 2011). However, such data is not available for most cases, and even when it is available, it is possible that the surface ejecta includes soil from both the liquefied stratum and overlying strata, as a result of the liquefied soil entraining material from overlying strata as it flows from the critical layer to the ground surface. An extreme example of this phenomenon occurred during the 1995 Kobe, Japan, earthquake where a soil stratum underlying a municipal solid waste dump liquefied. The resulting surface ejecta included soil from the critical layer and municipal solid waste that was carried to the surface by the liquefied soil (Bray, 2011).

For “no” cases, no soil ejecta is present, so comparing soil ejecta to boring samples is not an option for selecting the critical layer. Accordingly, for “no” cases, as well as “yes” cases where no information about the surface ejecta is available, critical layers typically are selected solely based on in-situ test data. However, investigators rarely describe the criteria used to select the critical layers for these cases. The few studies that do provide such details typically use existing CRR curves to evaluate liquefaction potential throughout the profile and the critical layer is defined as the layer with the lowest factor of safety against liquefaction, FS_{liq} (e.g., Moss et al., 2006; Kayen et al., 2013). In short, there is little to no consistency in how critical layers were selected among available case history databases, and the interpretation of many case histories may be biased due to the use of existing triggering curves to select the critical layers.

Once a critical layer is selected, representative soil properties of the layer must be defined, and often are expressed in terms of in-situ index test values. For the stress-based simplified procedure, soil properties for each case history are represented by a single, normalized in-situ index test value (e.g., SPT blow count corrected for hammer energy, effective confining stress, sampler configuration, rod length, borehole diameter, and soil fines content). When multiple in-situ index test values were measured in the critical layer (within a single boring/sounding or from multiple borings/soundings), judgment is required to select a representative value. For example, Liao and Whitman (1986) selected the lowest index test value measured in the critical layer as the representative value. In contrast, other studies averaged in-situ index test values to define a representative value (e.g., Cetin, 2000; Idriss and Boulanger, 2008). However, with this latter approach, the representative index test value can differ depending on whether the index test values are averaged first and then corrections are applied, or the corrections are applied to the individual values first and then the corrected values are averaged. The differences can be particularly significant for soils with high fines contents. Also, when an average index test value is selected as representative, the selected thickness of the critical layer becomes important because the measured index test values often vary with depth in a given stratum (e.g., Green et al., 2014; Boulanger and Idriss, 2014).

Proposed Approach to Selecting Critical Layers

The geologic setting often significantly influences the mode and severity of liquefaction manifestations (Youd, 1984), as local variability in sand properties largely depends on geologic setting. For example, hydraulic fracturing may occur as a result of liquefaction of a localized body of susceptible sand. However, major lateral spreading (i.e., displacement ≥ 1 m extending several tens of meters back from a free face) requires liquefaction to occur in a continuous, laterally-extensive stratum. Additionally, a highly variable or discontinuous profile (especially laterally) in proximity to a surficial fine-grained cap can introduce uncertainty in assessing which sand stratum actually liquefied. In turn, this scenario makes it virtually impossible to interpret a representative index test value. Braid-bar deposits – commonplace along rivers or abandoned river channels – are especially prone to this problem. In contrast, point-bar deposits are often relatively uniform for large distances (hundreds of meters laterally). As a result, the geologic setting, in conjunction with the severity of surficial liquefaction manifestations, must be considered when interpreting liquefaction case histories. Additionally, the depth, thickness, and density of the selected critical layer must be consistent with the observed liquefaction response.

Olson et al. (2005) and Green et al. (2005) proposed a set of guidelines for interpreting paleoliquefaction sites in the Central U.S. The guidelines proposed here are intended for interpreting modern liquefaction case histories. Integral to these guidelines is classifying the severity of the surficial liquefaction manifestations beyond just “yes” or “no.” Classes of liquefaction severity are “No Liquefaction,” “Minor Liquefaction,” “Moderate Liquefaction,” “Severe Liquefaction,” “Lateral Spreading,” and “Severe Lateral Spreading.” Table 1 provides quantitative metrics for each severity class proposed by Maurer et al. (2014) and used herein.

Table 1. Liquefaction severity classification criteria (Maurer et al., 2014).

Classification	Criteria
No Liquefaction	No surficial liquefaction manifestation or lateral spread cracking
Marginal Liquefaction	Small, isolated liquefaction features; streets had traces of ejecta or wet patches less than a vehicle width; < 5% of ground surface covered by ejecta
Moderate Liquefaction	Groups of liquefaction features; streets had ejecta patches greater than a vehicle width but were still passable; 5-40% of ground surface covered by ejecta
Severe Liquefaction	Large masses of adjoining liquefaction features, streets impassable due to liquefaction, >40% of ground surface covered by ejecta
Lateral Spreading	Lateral spread cracks were predominant manifestation and damage mechanism, but crack displacements < 200 mm
Severe Lateral Spreading	Extensive lateral spreading and/or large open cracks extending across the ground surface with > 200 mm crack displacement

Guidelines

1. Severe surficial liquefaction manifestation (e.g., extensive ground cracking and massive sand boils on the ground surface) requires a relatively thick, loose liquefiable stratum. The deeper the stratum, the thicker the layer must be for these features to manifest at the ground surface.
2. Moderate surficial liquefaction manifestation (e.g., moderate-sized ground cracking and moderate-sized sand boils on the ground surface) can result from a slightly thinner, slightly denser, and/or slightly deeper liquefiable stratum compared to severe manifestations.
3. Minor surficial liquefaction manifestation (e.g., limited ground cracking, limited surface ejecta, and/or limited water seepage at the ground surface) can result from: (1) a relatively loose, thin, deep layer severely liquefying; (2) a loose to medium dense, thick, shallow layer that generates large excess pore pressures but does not liquefy; or (3) a relatively dense, thick, shallow layer marginally liquefying. For these cases, the thickness of a loose stratum must increase as its depth below grade increases, or the density of a medium-dense stratum must decrease as its depth increases. Additionally, the surficial liquefaction manifestation can be significantly influenced by the characteristics of the non-liquefied strata in the profile and thus needs to be considered.
4. The critical layer associated with lateral spreading can be relatively thin, but its thickness must increase and/or density decrease as the volume surface ejecta or lateral spreading displacement increases. However, selection of the critical layer

should also consider the surface slope, free-face height, and lateral continuity of the liquefiable stratum relative to the lateral spread area.

The above guidelines do not explicitly consider variations of induced seismic stress with depth, although this is indirectly considered in selecting the critical layer. To assess the influence of seismic stress variations, the FS_{liq} should be computed using various liquefaction evaluation procedures to determine if there are any credible alternative critical layers. If alternatives are present, judgment must be used to select an appropriate critical layer. However, this is a secondary step, and the authors consider it different from using a particular liquefaction evaluation procedure to select case history critical layers, and then using the same case histories to validate the predictive capabilities of the same liquefaction evaluation procedure (or to invalidate the predictive capabilities of another liquefaction evaluation procedure). Below, two sites are detailed to illustrate the implementation of the proposed guidelines.

Example Case History Interpretations

The first example involves a site that was subjected to multiple earthquakes during the 2010-2011 Canterbury, New Zealand, Earthquake Sequence (CES). However, the authors focus on two episodes of shaking: the 2010 ($M_w 7.1$) Darfield and 2011 ($M_w 6.2$) Christchurch earthquakes. The site, designated as KAN-26, is located in a park along the Kaiapoi River in North Kaiapoi. Moderate surficial liquefaction manifestations formed during the Darfield earthquake, while minor surficial liquefaction manifestations formed during the Christchurch earthquake. Despite its proximity to the Kaiapoi River, there was no evidence of lateral spreading at this site, although severe lateral spreading occurred along other stretches of the river banks, including the river bank opposite to this site. Figure 1 presents profiles of cone penetration test (CPT) q_c , R_f , I_c , and D_r for KAN-26. The critical layers selected for the Darfield and Christchurch earthquakes are superimposed on the plots. The representative normalized penetration resistance (q_{c1Ncs}) for the critical layer for the Darfield earthquake is 103.0 atm (Idriss and Boulanger 2008 procedure), while $q_{c1Ncs} = 59.7$ atm for the Christchurch earthquake. As discussed by Green et al. (2014), in computing the representative q_{c1Ncs} values, corrections were applied to the measured values and the corrected values were then averaged. This approach is more correct technically than the averaging the measured values and then applying corrections to the averaged values.

As shown in Figure 1, different critical layers were selected for the two earthquakes to maintain consistency among the depth-thickness-density of the critical layers and the severity of liquefaction surface manifestations observed for each earthquake. The relatively loose and thin upper critical layer has a depth-thickness-density combination that is consistent with the minor surface manifestations observed during the Christchurch earthquake. Because it is relatively thin, it is doubtful that this layer could produce surface manifestations more severe than minor, in the absence of lateral spreading. As such, the more severe manifestations associated with the Darfield earthquake required the thicker (although deeper) critical layer identified in Figure 1.

This two-critical-layer interpretation also is supported by field observations. Ejecta associated with minor surface manifestations formed during the Christchurch earthquake were brown in color, which is evidence of oxidation and the development of iron oxide by-products resulting from exposure to oxygen via a fluctuating shallow groundwater table or from being a fill

material – both consistent with a shallow layer. (This layer was later confirmed as a layer of fill.) In contrast, the moderate liquefaction surface manifestations that formed during the Darfield earthquake included both brown and blue-gray sand ejecta, with the blue-gray sand remaining in a reducing atmosphere, sealed from oxygen by being below the groundwater table continuously, consistent with a deeper layer. For the KAN-26 site, simply selecting a critical layer based on the lowest penetration resistance or the lowest computed factor of safety against liquefaction, without considering the severity of surficial liquefaction manifestations, would have resulted in selecting only one critical layer (i.e., the relatively thin critical near-surface layer selected for the Christchurch earthquake) and an incomplete or even incorrect interpretation.

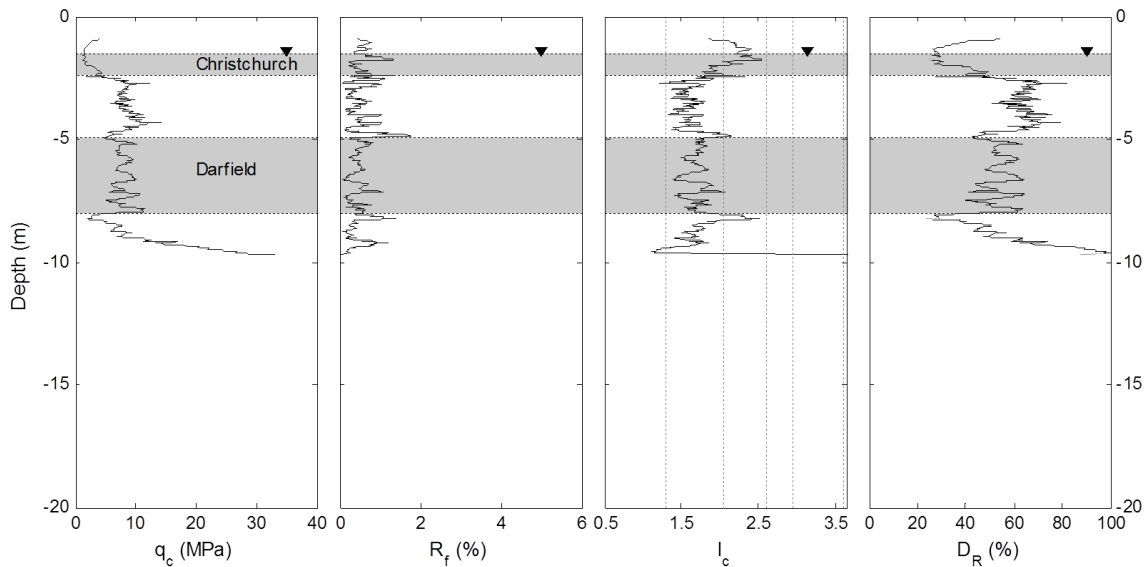


Figure 1. Measured CPT tip resistance (q_c), friction ratio (R_f), soil behavior type index (I_c), and estimated relative densities (D_R) with depth for Site KAN-26 with superimposed critical layers.

The second example involves a site located in the Wabash Valley region of the central U.S. that was subjected to shaking during a paleoearthquake that occurred ~6100 yr BP. The site, designated as Peankishaw Bend (PB), is located along a 4+ km-long bank exposure along the Wabash River that is at least 5 m high everywhere. Figure 2 shows a vertical section of the site, soil strata, boring locations and SPT blow counts, and ground surface and groundwater table elevations at the time of the earthquake (~6,100 yr BP). The bank at the site is clearly scoured by annual flooding, allowing numerous opportunities to examine the deposits for liquefaction effects (Obermeier, 2004). Two dikes that resulted from lateral spreading were observed at the site, one 0.15 m wide and the other 0.7 m wide. Aerial photos show that all granular deposits at the site were laid down as point-bar deposits, while the river was operating in a meandering mode (Obermeier et al., 1993). The plan-view pattern of scroll bars indicates that the ages of these deposits increases northward. Considering the deposit ages and field geologic interpretations, Obermeier (2004) hypothesized that lateral spreading developed by movement of a block of sediment, extending from the 0.7 m wide dike and going southward at least 75 m.

As shown in Figure 2, boring B2 is located near the 0.7 m-wide dike and boring B1 is located near the 0.15 m-wide dike. A considerable quantity of gravel was vented to the ground surface at

the location of the 0.7 m wide dike. Field observations over a number of years revealed that none of the strata above the groundwater table (ATE) had liquefied (Obermeier, 2004). Therefore the only plausible source stratum is the thick sand layer at a depth of about 5.2 m from the current ground surface. Olson et al. (2005) selected a representative index test value as the lowest value that is common among borings performed along the length of the lateral spread. Considering the SPT blow counts shown in Figure 2 (corrected and normalized per Youd et al. 2001), Olson et al. (2005) selected a representative SPT blow count of $N = 20$ ($N_{1,60cs} = 21.5$), at a depth of 8.5 m from the current ground surface (which corresponds to a depth of ~ 6.1 m from the ground surface at the time of the earthquake).

For the PB site, a single boring performed adjacent to the largest dike likely would have resulted in selecting $N = 7$ to 11 as the representative value for the critical layer (i.e., Boring B2 in Figure 2, depth of ~ 6.5 to 7.5 m from the current ground surface). However, the mode and severity of liquefaction (severe lateral spreading) required that the critical layer have significant lateral continuity. Taking this into consideration resulted in a very different interpretation of the case history, which was supported further by observations of the profile in sectional view – a rarity for modern liquefaction case histories.

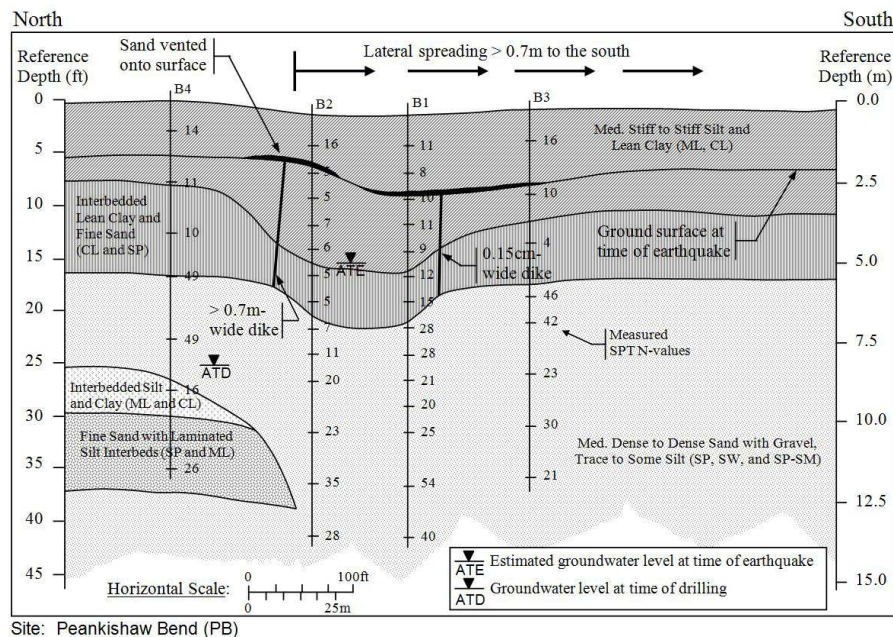


Figure 2. Representative vertical section of Site PB (adapted from Pond and Martin, 1996).

Conclusions

There is little consistency in how critical layers were selected for the compiled liquefaction case histories in existing databases, and the interpretation of many these case histories may be biased due to the use of existing triggering curves to select the critical layers. In this paper, the authors propose guidelines for interpreting liquefaction case histories that are based on consistency between the mode and severity of observed surficial manifestations and the characteristics of the identified critical layer. Two field case histories are used to illustrate the authors' proposed

guidelines. One of the case histories is of a site subject to multiple earthquakes during the 2010-2011 Canterbury, New Zealand, Earthquake Sequence. For this site, two different critical layers were selected: one for the 2010 Darfield earthquake, and one for the 2011 Christchurch earthquake. This two-critical-layer hypothesis was based on the characteristics of the layers and the severity of the surficial liquefaction manifestations. This hypothesis was validated by considering the characteristics of the liquefaction ejecta from the two events. The second case history is of a site that experienced severe lateral spreading during a paleoearthquake that occurred in the Wabash Valley of the central U.S. Here, the selected critical layer and representative in-situ index test value would have been very different if the mode and severity of liquefaction manifestation were not considered. Because the site is located adjacent to a river and the bank at the site was cleanly scoured by annual flooding, the site could be examined in sectional view numerous times over many years, with observations further supporting the authors' interpretation of this case history.

Acknowledgments

This study is based on work supported by the U.S. National Science Foundation (NSF) grants CMMI-1030564, CMMI-1407428, and CMMI-1435494. Additionally, several investigators were involved in the post-event documentation of the case histories presented above, to include Misko Cubrinovski, Liam Wotherspoon, Clint Wood, Brady Cox, Brendon Bradley, Steve Obermeier, Eric Pond, among others. The authors gratefully acknowledge both the funding and the efforts of others in performing the field documentation. However, any opinions, findings, and conclusions or recommendations expressed in this paper are those of the authors and do not necessarily reflect the views of NSF or any of the investigators mentioned herein.

References

- Boulanger RW, Idriss IM. *CPT and SPT based liquefaction triggering procedures*. Report No. UCD/CGM-14/01, Center for Geotechnical Modeling, Civil & Environmental Eng. Dept., Univ. of California, Davis, CA, 2014, 134
- Bray J. Personal Communication with R. Green. 2011.
- Cetin KO, Seed RB, Moss RES, Der Kiureghian AK, Tokimatsu K, Harder LF, Kayen RE. *Field performance case histories for SPT-based evaluation of soil liquefaction triggering hazard*, Geotechnical Engineering Research Report No. UCB/GT-2000/09, Civil Engineering Department, University of California at Berkeley. 2000.
- Green RA, Obermeier SF, Olson SM. Engineering geologic and geotechnical analysis of paleoseismic shaking using liquefaction effects: field examples. *Engineering Geology* 2005; **76**: 263-293.
- Green RA, Wood C, Cox B, Cubrinovski M, Wotherspoon L, Bradley B, Algie T, Allen J, Bradshaw A, Rix G. Use of DCP and SASW tests to evaluate liquefaction potential: predictions vs. observations during the recent New Zealand earthquakes. *Seismological Research Letters* 2011; **82**(6): 927-938.
- Green RA, Cubrinovski M, Cox B, Wood C, Wotherspoon L, Bradley B, Maurer B. Select liquefaction case histories from the 2010-2011 Canterbury earthquake sequence. *Earthquake Spectra* 2014; **30**(1): 131-153.
- Idriss IM, Boulanger RW. *Soil liquefaction during earthquakes*. Monograph MNO-12, Earthquake Engineering Research Institute, Oakland, CA, 2008; 261 pp.
- Kayen R, Moss R, Thompson E, Seed R, Cetin K, Der Kiureghian A, Tanaka Y, Tokimatsu K. Shear-wave velocity-based probabilistic and deterministic assessment of seismic soil liquefaction potential. *J. Geotech. Geoenviron. Eng.* 2013; **139**(3): 407-419.
- Liao SSC, Whitman RV. *A Catalog of liquefaction and non-liquefaction occurrences during earthquakes*. Research

Report, Department of Civil Engineering, Massachusetts Institute of Technology, Cambridge, MA.1986.

Maurer BW, Green RA, Cubrinovski M, Bradley BA. Evaluation of the liquefaction potential index for assessing liquefaction hazard in Christchurch, New Zealand. *J. Geotech. Geoenviron. Eng.* 2014; **140**(7).

Moss RES. *CPT-based probabilistic assessment of seismic soil liquefaction initiation*. Ph.D. Dissertation, University of California Berkeley. 2003.

Moss RES, Seed RB, Kayen RE, Stewart JP, Der Kiureghian A, Cetin KO. CPT-based probabilistic and deterministic assessment of in situ seismic soil liquefaction potential. *J. Geotech. Geoenviron. Eng.* 2006; **132**(8): 1032-1051.

Obermeier SF. Personal Communication with R. Green and S. Olson. 2004.

Obermeier SF, Martin II JR, Frankel AD, Youd TL, Munson PJ, Munson CA, Pond EC. Liquefaction evidence for one or more strong Holocene earthquakes in the Wabash Valley of southern Indiana and Illinois, *U.S. Geological Survey Professional Paper* 1536, 27 p.1993.

Olson SM, Green RA, Obermeier SF. Engineering geologic and geotechnical analysis of paleoseismic shaking using liquefaction effects: a major updating. *Engineering Geology* 2005; **76**: 235-261.

Pond EC, Martin II JR. *Seismic parameters for the central United States based on paleoliquefaction evidence in the Wabash Valley*. Final Report Submitted to the USGS, August, 583 p. 1996.

Seed HB, Idriss IM. Simplified procedure for evaluating soil liquefaction potential. *Journal of the Soil Mechanics and Foundation Division* 1971; **97**(SM9): 1249-1273.

Seed HB, Tokimatsu K, Harder Jr LF, Chung R. *Influence of SPT procedures in soil liquefaction resistance evaluations*. Report No. UCB/EERC-84/15, Earthquake Eng. Research Center, Univ. of California Berkeley 1984.

Stark TD, Olson SM. Liquefaction resistance using CPT and field case histories. *J. Geotech. Eng.* 1995; **121**(12): 856-869.

Tokimatsu K, Yoshimi Y. Empirical correlation of soil liquefaction based on SPT N-value and fines content. *Soils and Foundations* 1983; **23**(4): 56-74.

Whitman RV. Resistance of soil to liquefaction and settlement. *Soils and Foundations* 1971; **11**(4): 59-68.

Yegian MK, Vitelli BM. *Probabilistic analysis for liquefaction*, Report No. CE-81-1, Dept of Civil Engineering, Northeastern University, Boston, MA, 1981.

Youd TL. Geologic effects – liquefaction and associated ground failure. *Proc., Geologic and Hydrologic Hazards Training Program*, USGS Open File Report 84-760, US Geological Survey, US Dept. of the Interior, 210-232. 1984.

Youd TL, Idriss IM, Andrus RD, Arango I, Castro G, Christian JT, Dobry R, Finn WDL, Harder Jr LF, Hynes ME, Ishihara K, Koester JP, Liao SSC, Marcuson III WF, Martin GR, Mitchell JK, Moriwaki Y, Power MS, Robertson PK, Seed RB, Stokoe II KH. Liquefaction resistance of soils: summary report from the 1996 NCEER and 1998 NCEER/NSF workshops on evaluation of liquefaction resistance of soils. *J. Geotech. Geoenviron. Eng.* 2001; **127**(4): 297-313.